

AperTO - Archivio Istituzionale Open Access dell'Università di Torino

## Hemopexin counteracts systolic dysfunction induced by heme-driven oxidative stress

### **This is the author's manuscript**

*Original Citation:*

*Availability:*

This version is available <http://hdl.handle.net/2318/1634491> since 2017-05-16T11:27:25Z

*Published version:*

DOI:10.1016/j.freeradbiomed.2017.04.003

*Terms of use:*

Open Access

Anyone can freely access the full text of works made available as "Open Access". Works made available under a Creative Commons license can be used according to the terms and conditions of said license. Use of all other works requires consent of the right holder (author or publisher) if not exempted from copyright protection by the applicable law.

(Article begins on next page)

This Accepted Author Manuscript (AAM) is copyrighted and published by Elsevier. It is posted here by agreement between Elsevier and the University of Turin. Changes resulting from the publishing process - such as editing, corrections, structural formatting, and other quality control mechanisms - may not be reflected in this version of the text. The definitive version of the text was subsequently published in *FREE RADICAL BIOLOGY & MEDICINE*, 108, 2017, 10.1016/j.freeradbiomed.2017.04.003.

You may download, copy and otherwise use the AAM for non-commercial purposes provided that your license is limited by the following restrictions:

- (1) You may use this AAM for non-commercial purposes only under the terms of the CC-BY-NC-ND license.
- (2) The integrity of the work and identification of the author, copyright owner, and publisher must be preserved in any copy.
- (3) You must attribute this AAM in the following format: Creative Commons BY-NC-ND license (<http://creativecommons.org/licenses/by-nc-nd/4.0/deed.en>), 10.1016/j.freeradbiomed.2017.04.003

The publisher's version is available at:

<http://linkinghub.elsevier.com/retrieve/pii/S0891584917301946>

When citing, please refer to the published version.

Link to this full text:

<http://hdl.handle.net/2318/1634491>

**Hemopexin counteracts systolic dysfunction induced by heme-driven oxidative stress**

Giada Ingoglia<sup>1</sup>, Can Martin Sag<sup>2</sup>, Nikolai Rex<sup>2</sup>, Lucia De Franceschi<sup>3</sup>, Francesca Vinchi<sup>4</sup>, James Cimino<sup>1</sup>, Sara Petrillo<sup>1</sup>, Stefan Wagner<sup>2</sup>, Klaus Kreitmeier<sup>2</sup>, Lorenzo Silengo<sup>1</sup>, Fiorella Altruda<sup>1</sup>, Lars S. Maier<sup>2</sup>, Emilio Hirsch<sup>1</sup>, Alessandra Ghigo<sup>1</sup> and Emanuela Tolosano<sup>1</sup>

<sup>1</sup>Dept. Molecular Biotechnology and Health Sciences, University of Torino, Torino, Italy

<sup>2</sup>Dept. Internal Medicine II, University Hospital Regensburg, Regensburg, Germany

<sup>3</sup>Dept. Medicine, Università degli Studi di Verona–Azienda Ospedaliera Universitaria Integrata Verona, Verona, Italy

<sup>4</sup>Heidelberg University Hospital / EMBL Heidelberg, Heidelberg, Germany

**Corresponding author:**

Emanuela Tolosano, PhD  
Molecular Biotechnology Center  
Dept. Molecular Biotechnology and Health Sciences  
Via Nizza 52  
10126 Torino, Italy  
Phone: +39-011-6706423  
Fax: +39-011-6706432  
email: [emanuela.tolosano@unito.it](mailto:emanuela.tolosano@unito.it)

**Abstract**

Heart failure is a leading cause of morbidity and mortality in patients affected by different disorders associated to intravascular hemolysis. The leading factor is the presence of pathologic amount of pro-oxidant free heme in the bloodstream, due to the exhaustion of the natural heme scavenger Hemopexin (Hx). Here, we evaluated whether free heme directly affects cardiac function, and tested the therapeutic potential of replenishing serum Hx for increasing serum heme buffering capacity.

The effect of heme on cardiac function was assessed *in vitro*, on primary cardiomyocytes and H9c2 myoblast cell line, and *in vivo*, in Hx<sup>-/-</sup> mice and in genetic and acquired mouse models of intravascular hemolysis. Purified Hx or anti-oxidants N-Acetyl-L-cysteine and  $\alpha$ -tocopherol were used to counteract heme cardiotoxicity.

In mice, Hx loss/depletion resulted in heme accumulation and enhanced reactive oxygen species (ROS) production in the heart, which ultimately led to severe systolic dysfunction. Similarly, high ROS reduced systolic Ca<sup>2+</sup> transient amplitudes and fractional shortening in primary cardiomyocytes exposed to free heme. In keeping with these Ca<sup>2+</sup> handling alterations, oxidation and CaMKII-dependent phosphorylation of Ryanodine Receptor 2 were higher in Hx<sup>-/-</sup> hearts than in controls. Administration of anti-oxidants prevented systolic failure both *in vitro* and *in vivo*. Intriguingly, Hx rescued contraction defects of heme-treated cardiomyocytes and preserved cardiac function in hemolytic mice.

We show that heme-mediated oxidative stress perturbs cardiac Ca<sup>2+</sup> homeostasis and promotes contractile dysfunction. Scavenging heme, Hx counteracts cardiac heme toxicity and preserves left ventricular function. Our data generate the rationale to consider the therapeutic use of Hx to limit the cardiotoxicity of free heme in hemolytic disorders.

**Keywords:** Heme, Hemopexin, ROS, Heart, Systolic function

## Introduction

Heart failure, one of the leading causes of morbidity and mortality worldwide, is a multifactorial complex disorder that leads to a disturbance of the normal pump activity of the heart to meet the metabolic demands of the body [1]. Excess production of reactive oxygen species (ROS) has been implicated in progression of chronic heart failure as well as in other cardiovascular disorders including ischemia-reperfusion injury and cardiovascular complications of hemolytic diseases [2-7].

Free heme is a strong driver of oxidation and it has been shown to affect the function of various cell components within the cardiovascular system [8]. Heme promotes endothelial dysfunction by inducing the expression of adhesion molecules and reducing nitric oxide (NO) availability, which causes vasoconstriction [9-14]. Moreover, heme-derived ROS induce the proliferation of smooth muscle cells, that participate in vasculopathy associated with atherosclerosis and hypertension [15]. Finally, heme causes oxidant damage to thick filament proteins, leading to contractile dysfunction in human cardiomyocytes *in vitro* [16].

Under physiologic conditions, heme levels are maintained in plasma at very low concentration (0.2  $\mu\text{mol/L}$ ) [17]. However, in pathologic conditions associated with intravascular hemolysis such as hemolytic anemias (i.e. hemoglobinopathies or G6PD deficiency), heme levels rise up to 20-50  $\mu\text{mol/L}$  [17]. Interestingly,  $\beta$ -thalassemia intermedia, a paradigmatic disorder of chronic hemolysis with increased free heme, has been associated with systolic and diastolic dysfunction, leading to the development of heart failure, which is a life-threatening complication in these patients [18]. Although progresses have been made in the knowledge of the pathogenesis of organ damage related to hemolytic disorders, the molecular mechanisms leading to impaired heart function are still largely unknown and the potential contribution of free heme-driven oxidative stress on left ventricular dysfunction has not been clarified yet.

Hemopexin (Hx) is a plasma acute phase glycoprotein produced by the liver and able to bind an equimolar amount of heme with high affinity [19]. Upon heme binding, the Hx-heme complex is taken up by the liver and heme catabolized by heme oxygenases [19]. In this way, Hx works as a plasma buffering system to keep circulating heme at very low concentration. Nevertheless, during sustained hemolysis, Hx is fully saturated and free heme levels rise, leading to tissue oxidative damage [9, 20-22]. Recent studies have highlighted the potential therapeutic role of exogenous Hx in mouse models of sickle cell disease. In sickle cell disease mice, exogenous Hx markedly reduces inflammatory vasculopathy, prevents the development of severe acute vaso occlusive events and improves cardiac function [9, 23, 24]. Given these data, we asked whether the beneficial effect of Hx on the cardiovascular system might be due not only to preservation of vascular homeostasis but also to specific effects on the heart.

Here, we show that heme impairs calcium homeostasis in cardiomyocytes, and in turn impairs cardiac contractility, both *in vitro* and in *in vivo* models of hemolytic disorders. Hx preserves systolic function by preventing heme-driven ROS production and Ca<sup>2+</sup> mishandling in cardiomyocytes. We propose non-hemopexin bound heme (NHBH) as new factor contributing to cardiotoxicity in chronic hemolytic diseases, such as  $\beta$ -thalassemia, together with free pathologic iron (non-transferrin bound iron, NTBI). Our results support the use of Hx as a therapeutic option to prevent severe heart complication related to NHBH in chronic hemolytic diseases.

## **Methods**

### **Mouse neonatal cardiomyocyte isolation and culture**

Spontaneously beating neonatal cardiac myocytes were prepared from hearts of 1- to 2-day-old mouse pups. Pups were anesthetized by hypothermia, sacrificed via decapitation and hearts were removed. Atria were cut off and ventricles were minced and pre-digested overnight at 4°C in

calcium-free HEPES-buffered Hanks' solution, pH 7.4, containing 0.5 mg/ml trypsin (USB Corporation, Cleveland, Ohio). The following day, ventricles were incubated at 37°C for 5 minutes in calcium-free HEPES buffered Hanks' solution, pH 7.4, containing 330 U/ml collagenase type II (Worthington Biochemical, Lakewood, NJ). The digestion step was repeated 3-4 times. To reduce the contribution of non-myocardial cells, cells were pre-plated for 1h. The myocyte-enriched cells remaining in suspension were plated on 35-mm tissue culture dishes at a density of  $1.5 \times 10^5$  cells per dish. Culture dishes were pre-coated with a solution of 0.2% gelatin (Sigma-Aldrich, Saint Louis, MO) and 15 mg/mL fibronectin for 30 minutes. Myocytes were cultured in a Dulbecco's modified Eagle's medium/Medium 199 (Gibco, Carlsbad, CA) mix containing 10% horse serum, 5% fetal bovine serum, and 5 mmol/L penicillin/streptomycin (Gibco, Carlsbad, CA).

The rat-derived myoblast cell line H9c2 (ATCC CRL-1446™) was cultured in Dulbecco's modified Eagle's medium/Medium 199 (Gibco, Carlsbad, CA) containing 10 % fetal bovine serum, and 5 mmol/L penicillin/streptomycin (Gibco, Carlsbad, CA).

### **Heme treatment**

Hemin chloride was dissolved in dimethyl sulfoxide to obtain a 4-mmol/L stock solution, diluted, and mixed 1:1 with human serum albumin (CSL Behring, Switzerland) or Hx (CSL Behring, Switzerland). Cardiomyocytes were treated with albumin-heme, Hx-heme or heme 5 to 10  $\mu\text{mol/L}$  in culture medium until 8 hours. After treatment, cells were washed twice. H9c2 cells were treated with Hx-heme or heme 5 to 10  $\mu\text{mol/L}$  in culture medium until 8 hours. After treatment, cells were washed twice.

### **Mice and Treatments**

C57BL/6 Hx<sup>-/-</sup> mice and Hbb<sup>th3/+</sup> mice as a model of  $\beta$ -thalassemia were described previously [20, 25-29]. All mice were housed in our animal facility, with a 12-h dark/light cycle and access to standard laboratory chow and tap water ad libitum. Sex- and age-matched C57BL/6 wild-type mice were used as controls.

C57BL/6 wild-type mice were administered intraperitoneally (i.p.) with 25 mg/kg phenylhydrazine (PHZ, Sigma-Aldrich, Saint Luis, USA) twice a week for 4 weeks. PHZ-treated mice were injected i.p. with 160 mg/Kg Hx dissolved in PBS or 400 mg/kg  $\alpha$ -tocopherol (Sigma-Aldrich) dissolved in corn oil or with vehicle on the day of PHZ injection. Control animals were injected with PBS or corn oil. Animals were anesthetized by intramuscular injection of Zoletil (80 mg/kg)/Xylazine (16 mg/kg), and serum and tissue samples were collected and kept frozen until analysis.

All animal procedures were performed conform the guidelines from Directive 2010/63/EU of the European Parliament on the protection of animals used for scientific purposes. This study was approved by the Italian regulatory authority (approval reference number 87/2015-PR).

### **Heme Content**

Heme content in cells and tissues was quantified fluorometrically by the method of Sassa[30, 31]. Briefly, tissues or cells were homogenized in phosphate buffer saline (PBS) and protein content was determined by using the Bio-Rad protein assay system (Bio-Rad, Munchen, Germany). Ten ug of protein samples were incubated with 0.5 mL of 2 M Oxalic Acid (Sigma-Aldrich) at 95°C for 30 min. Samples were subsequently centrifuged at 14000 rpm for 5 min. Fluorescence emission in the supernatant was determined spectrofluorimetrically (Glomax, Promega Italia). Excitation and emission wavelengths were set at 405 and 662 nm, respectively. The background was evaluated by measuring fluorescence in non-boiled samples.



### **Quantitative Real-Time Polymerase Chain Reaction (qRT-PCR)**

Total RNA, from cells or tissues, was extracted using Pure Link RNA Mini Kit (Ambion, Life Technologies Italia, Milano, Italy). One  $\mu\text{g}$  total RNA was reverse transcribed using M-MLV reverse transcriptase and random primers (Life Technologies Italia). qRT-PCR was performed on a 7300 Real Time PCR System (Applied Biosystems, Life Technologies Italia). Primers and probes were designed using the ProbeFinder software (<http://www.roche-applied-science.com>). All results were normalized to 18S mRNA.

### **Protein Extraction and Western Blotting**

Tissue and cell proteins were extracted as reported [20] and concentration was determined using the Bio-Rad protein assay system (Bio-Rad, Munich, Germany). Fifty  $\mu\text{g}$  total protein or 0.25  $\mu\text{L}$  mouse serum in 8  $\mu\text{L}$  of Laemly Buffer were separated on 4%, 8% or 12% sodium dodecyl sulfate polyacrylamide gel electrophoresis and analyzed by Western blotting using antibodies against HO-1 (dilution 1:300, Enzo Life Sciences), Tfr1 (dilution 1:1000, Invitrogen), ox-CAMKII (dilution 1:1000, Gene Tex), tot-CAMKII (dilution 1:1000, Cell Signaling), RYR2 pSer 2814 (dilution 1:2500, Badrilla), total RYR2 (dilution 1:5000, Thermo Scientific), PLB pThr17 (dilution 1:1000, Badrilla), total PLB (1:1000, Merck Millipore), Hx (1:1000)[20], N-Tyr (1:1000, Merck Millipore).

### **RyR2 oxidation**

To detect RyR2 protein oxidation, hearts were homogenized in 120 mmol/L NaCl, 50 mmol/L Tris-HCl (pH 8.0) and 1% Triton X-100, supplemented with protease and phosphatase inhibitors. After 30 min incubation on ice, lysates were centrifuged at 3000 rpm for 5 min at 4°C and immunoprecipitated. Four mg of pre-cleared extracts were incubated with 20  $\mu\text{L}$  of protein G-Sepharose (Amersham Biosciences, Buckinghamshire, UK) and 4  $\mu\text{g}$  of anti-RYR2 antibody (Thermo

Scientific), for 2 h at 4°C. Immunoprecipitates were washed, treated with 2, 4-dinitrophenyl (DNP) hydrazine, separated on 4% SDS-PAGE and transferred onto PVDF membranes. The RYR2 DNP-derivatized carbonyls were detected using an OxyBlot Protein Oxidation Detection Kit (Merck Millipore); total RYR2 was detected with an anti-RyR2 antibody (Thermo Scientific).

### **ROS Production Assay**

Accumulation of ROS in heart homogenates or cells was assessed by using the oxidant-sensitive fluorescent dye 2',7'-dichlorodihydrofluorescein diacetate (H2DCFDA; Molecular Probes, Inc., Eugene, OR) as previously described[32]. Heart homogenates or cell extracts were incubated with 5µM H2DCFDA in phosphate buffered saline (PBS) or in serum-free medium, respectively, for 30 min at 37 °C under 5% CO<sub>2</sub> atmosphere. Fluorescence was recorded at excitation and emission wavelengths of 485 nm and 530 nm respectively, by a fluorimeter plate reader (Promega). The background fluorescence caused by PBS or medium and DCF was subtracted from the total fluorescence in each well generated by cells in presence of DCF. Fluorescence intensity was expressed as arbitrary fluorescence units/mg protein.

Following incubation for 6 h, adult rat cardiomyocytes media was discarded and replaced with the ROS sensitive fluorescent dye CM-H2DCFDA (at 10 µM, Invitrogen, USA). For ROS measurements, cells were excited at 485±15 nm on a Nikon Eclipse TE2000-U inverted microscope which was provided with a fluorescence detection system (ION OPTIX, Milton, MA, USA). Emitted fluorescence was collected at 535±20 nm for only 10 s every min to prevent photooxidation of the dye[33].

### **Lipid Peroxidation Assay**

Lipid peroxidation from tissue extracts was measured with the colorimetric assay kit Bioxytech LPO-586 from Oxis International (Portland, OR) according to the manufacturer's instructions.

### **Immunohistochemistry and histology**

Hearts were fixed in 10% formalin overnight at room temperature and embedded in paraffin. Microtome sections, 5- $\mu$ m thick, were incubated overnight with anti-HO-1 (Enzo Life Sciences) or anti- CD18 (Biolegend) antibody, both diluted 1:100, followed by biotin-conjugated secondary antibody. For collagen quantification, sections were stained with Picrosirius Red[34]. The sections were visualized on an Olympus BH-2 microscope, coupled to an Olympus camera. Collagen content was calculated as a percentage of the red-stained area *per* section by using Image J program.

### **Echocardiography**

Transthoracic echocardiography was performed with a small animal high-resolution imaging system (VeVo2100, VisualSonics, Inc, Toronto, Canada) equipped with a 22-55 MHz transducer (MicroScan Transducers, MS500D)12. The mice, anesthetized by isoflurane (2%) inhalation and maintained by mask ventilation (isoflurane 1%), were placed in a shallow left lateral decubitus position, with strict thermoregulation (37 $\pm$ 1°C) to optimize physiological conditions and reduce hemodynamic variability. Fur was removed from the chest by application of a cosmetic cream to gain a clear image. Echocardiographic parameters were measured at the level of the papillary muscles in the parasternal short-axis view (M mode). LV fractional shortening was calculated as follows:  $FS = ((LVEDD - LVESD) / LVEDD) \times 100$ , where LVFS indicates LV fractional shortening; LVEDD, LV end-diastolic diameter; and LVESD, LV end-systolic diameter. LV ejection fraction was calculated automatically by the echocardiography system. All measurements were averaged on 5 consecutive cardiac cycles per experiment and cardiac function was assessed when heart rate was 450-500 bpm.

### **Adult rat cardiomyocyte isolation and culture**

A modified protocol for rat myocytes isolation[35] was used. Adult 8-10 week old Sprague dawley rats (Janvier labs) were anaesthetized with isoflurane (2%) (Abbott, Wiesbaden, Germany). Afterwards, hearts were carefully excised and mounted on a Langendorff-perfusion apparatus, and subsequently perfused for 3 min with nominal Ca free solution. Next, the heart was perfused for  $\approx$ 15 min with an "enzyme solution" containing (in mmol/L) NaCl 113, KCl 4.7,  $\text{KH}_2\text{PO}_4$  0.6,  $\text{Na}_2\text{HPO}_4 \times 2 \text{H}_2\text{O}$  0.6,  $\text{MgSO}_4 \times 7 \text{H}_2\text{O}$  1.2,  $\text{NaHCO}_3$  12,  $\text{KHCO}_3$  10, HEPES 10, Taurine 30, Glucose 5.5, BDM 10, and  $\text{CaCl}_2$  0,0125, (all Roth, Karlsruhe, Germany), Liberase TM (1,5 mg, Roche, Mannheim, Germany), Trypsin 2,5%, (180  $\mu\text{l}$ , Gibco, Paisley, UK). After digesting the extracellular matrix up to the point of visible tissue solution, the heart was transferred into a glass basin that was filled with an enzyme-free "stop solution" that contained the same ingredients as the enzyme solution without the enzyme, but with BCS 10%. The atria were afterwards carefully separated from the ventricles and discarded. Subsequently, the ventricles were cut with preparatory scissors into small pieces of tissue. The cell suspension was filtered through a nylon gaze. After sedimentation of the tissue, stop solution was removed and replaced with a second enzyme free solution containing 5% BCS. Using this solution, Ca reintroduction was performed by stepwise increasing [Ca] from 0.1-1.2 mmol/L. Ca loaded cells were afterwards resuspended in Ca containing "cell culture media" consisting of M199 (Sigma-Aldrich) plus 1% Penicillin/Streptomycin and 1% Insulin-Transferrin-Streptomycin and transferred into Laminin-coated culture dishes. Hemin (H651-9, Frontier Scientific) as diluted in PBS to achieve a concentration of 50 $\mu\text{M}$  was added at 5  $\mu\text{M}$  vs. PBS control (vehicle) to the culture dish. In an independent set of experiments, an equal volume of 50  $\mu\text{M}$  heme solution was mixed with a 50  $\mu\text{M}$  Hx solution and incubated for 1 hour at 37 degrees in the dark, in order to form a Hx-Heme complex. Hemopexin-Heme solution was similarly added to an according culture dish at 5  $\mu\text{M}$ . In some experiments, N-Acetyl-L-cysteine (NAC, A7250 from Sigma-Aldrich) was added at 10 mM to heme-treated cells. Cell were afterwards cultured for 6 h at 37°C in darkness.

## Ca<sup>2+</sup> Measurements

Following incubation for 6 h, cell culture media was discarded and replaced with the Ca<sup>2+</sup> sensitive fluorescent dye Fura-2 AM (at 10  $\mu$ M, Invitrogen, USA). For Ca<sup>2+</sup> measurements, cells were excited at 340 nm and 380 nm and emitted fluorescence was collected at 510 nm. Ca<sup>2+</sup> transient amplitude was assessed as the 340/380 nm fluorescence ratio (F<sub>340nm</sub>/F<sub>380nm</sub> in ratio units, r.u.) after subtraction of background fluorescence at each excitation wavelength[33]. Myocytes were field-stimulated at 20 $\pm$ 4 V at 1 Hz for ~5 min until steady-state conditions were achieved. Myocytes were superfused with an experimental "normal Tyrode's (NT)" solution containing (in mmol/L) NaCl 140, KCl 4, glucose 10, HEPES 5, MgCl<sub>2</sub> 1, CaCl<sub>2</sub> 1.2, which has supplemented with PBS (vehicle) or hemin (at 5  $\mu$ M) at 22°C (pH 7.4). Red light transillumination was used to visualize myocytes sarcomeres.

## Statistical Analysis

Results were expressed as mean $\pm$ SEM. Prism software (GraphPad software Inc, La Jolla, CA) was used for statistical analysis. Comparisons between 2 groups were performed with 2-sided Welch t tests and among >2 groups with 1- or 2-way ANOVA followed by the Bonferroni post-test. A value of  $P < 0.05$  was considered significant.

## Results

### **Hemopexin protects neonatal cardiomyocytes from heme accumulation and ROS production**

Recently, we showed that, by scavenging heme, Hx prevents heme accumulation in endothelial and immune cells, thus limiting heme toxicity [9, 36]. To evaluate whether cardiomyocytes (CMs) may also be affected by pathologic free heme, we treated mouse neonatal CMs with 10  $\mu$ M heme, in presence of either Hx or Albumin (a low affinity heme-binding protein [17]).

Hx-heme-treated CMs were protected from heme accumulation, compared to cells treated with albumin-heme or heme alone (Figure 1A), indicating that Hx prevents heme entry in cardiac cells. Consistently, the mRNA and protein levels of the heme-degrading enzyme Heme Oxygenase (HO)-1 were significantly more elevated in cells treated with either albumin-heme or heme alone compared to cells treated with Hx-heme (Figure 1B, C). These results were confirmed in the H9c2 myoblast cell line treated with Hx-heme or heme alone (see Figure 2 in [37]). Moreover, in CMs the heme-mediated induction of the iron exporter Ferroportin (Fpn) was abrogated by Hx treatment while the down-regulation of the iron importer Transferrin receptor 1 (TfR1) was significantly reduced by Hx (see Figure 3 in [37]) further indicating that Hx limits heme-iron accumulation within the cell. Consistently, Hx treatment blunted heme-mediated induction of the heme exporter Feline Leukemia Virus subgroup C Receptor 1 (Flvcr1) [31, 38, 39] in H9c2 cells (see Figure 3 in [37]). Taken together, these data demonstrate that Hx prevents/limits heme accumulation in CMs.

Being heme a well-known pro-oxidant agent [17], we then evaluated ROS levels in CMs exposed to heme alone or bound to either Hx or albumin. In the presence of Hx-heme complexes, CMs were protected from ROS formation, if compared to CMs treated with either albumin-heme complexes or heme alone (Figure 1D). Staining of CMs with a fluorescent probe for specific detection of mitochondrial superoxide (Mito-sox) confirmed lower oxidative stress in cells exposed to Hx-heme than in those exposed to albumin-heme or heme alone (Figure 1E). Consistently, the mRNA levels of Glutathione reductase (Gsr),  $\gamma$ -Glutamylcysteine synthetase ( $\gamma$ -Gcs) and thioredoxin reductase (Thio red), anti-oxidant systems important in resistance of cardiac cell to oxidative damage [40, 41], were increased to a higher extent in CMs treated with either albumin-heme or heme alone, compared to cells treated with Hx-heme (Figure 1F and see Figure 3 in [37]). The data were reproduced in H9c2 cells in which we were also able to demonstrate that Hx limits protein nitrosylation, another hallmark of cellular oxidative damage (see Figure 2 in [37]).

Taken together, these data demonstrate that Hx protects cardiac cells against heme accumulation and related oxidative stress.

### **Hemopexin prevents heme-driven oxidative stress in the heart**

To assess whether the protective role of Hx observed *in vitro* is relevant also *in vivo*, we took advantage of Hx knockout (Hx<sup>-/-</sup>) mice [25]. 3 month-old Hx<sup>-/-</sup> mice showed a higher content of heme in the heart than age-matched wild-type animals (Figure 2A). Consistently, HO-1 mRNA and protein levels were higher in hearts from Hx<sup>-/-</sup> mice than in controls (Figure 2B). Immunohistochemistry for HO-1 on heart sections indicated higher HO-1 expression in cardiomyocytes from Hx<sup>-/-</sup> mice than in wild-type animals (Figure 2B). Moreover, the mRNA levels of Fpn and Flvcr1a were increased in Hx<sup>-/-</sup> mice, whereas those of the iron importers Divalent Metal Transporter 1 (Dmt1) and Tfr1 were decreased (see Figure 4 in [37]). TFR1 down-modulation was also confirmed at the protein level (see Figure 4 in [37]).

To evaluate the oxidative stress in the heart, we analysed ROS levels and lipid peroxidation in Hx<sup>-/-</sup> and wild-type mice. Both ROS and lipid peroxidation were increased in the heart of Hx<sup>-/-</sup> mice compared to that of wild-type animals (Figure 2C, D). Consistently, the oxidative stress responsive gene Gsr was up-regulated in the heart of Hx<sup>-/-</sup> mice compared to wild-type animals (Figure 2E). Altogether, these data demonstrate a critical role for Hx in preventing heme-driven oxidative stress in the myocardium.

### **Hemopexin prevents heme overload-induced heart dysfunction**

To evaluate whether heme-driven oxidative stress impairs heart function, we performed echocardiography on Hx<sup>-/-</sup> and control mice. Cardiac contractility was severely impaired in 3 month-old Hx<sup>-/-</sup> mice compared to wild-type controls, as evidenced by significantly lower fractional

shortening (FS) and ejection fraction (EF) (Figure 3A-C). Notably, in  $Hx^{-/-}$  mice, systolic dysfunction worsened at 6 months of age (Figure 3A-C), indicating an age-dependent progression of ventricular dysfunction, which was not associated to left side chamber dilation or left ventricular hypertrophy (Table 1). No evidences of collagen deposition or leukocyte infiltration in  $Hx^{-/-}$  heart were observed, despite a slight transcriptional up-regulation of pro-inflammatory Interleukin 6 (IL-6) and tumor necrosis factor- $\alpha$  (TNF- $\alpha$ ) (see Figure 5 in [37]). To dissect the cardiotoxic effect of free heme, we evaluated systolic function in  $Hbb^{th3/+}$  mice used as model of non-transfusion dependent  $\beta$ -thalassemia intermedia [29, 42]. Interestingly, a similar systolic dysfunction was observed in  $\beta$ -thalassemic mice (Figure 3D-F and Table 2) that are hallmarked by a high rate of intravascular hemolysis as evidenced by Hx depletion in serum, HO-1 induction at mRNA and protein level in the heart and altered cardiac expression of iron and anti-oxidant genes (see Figure 6 in [37]). These data further strength the link between plasma Hx depletion/heme overload and defective heart function.

Finally, to demonstrate that exogenous heme is the main responsible for systolic dysfunction when Hx is lost, we performed echocardiography in wild-type mice treated with the hemolytic agent phenylhydrazine (PHZ). PHZ treatment resulted in an almost complete depletion of serum Hx and in an up-regulation of heme- and oxidative stress-responsive genes in the heart (see Figure 7 in [37]). Consistently with our observations in both  $Hx^{-/-}$  mice and  $\beta$ -thalassemic mice, a significant reduction of FS and EF was observed in PHZ-treated wild-type animals (Figure 3G-I).

These data collectively indicate that heart free heme accumulating when Hx is lost is responsible for systolic dysfunction.

### **Hemopexin prevents heme overload-induced $Ca^{2+}$ mishandling**



In a next step, we aimed to investigate the cellular mechanisms underlying reduced systolic function associated with heme overload and oxidative stress, observed in Hx<sup>-/-</sup> mice. Since oxidative stress is known to directly impair Ca<sup>2+</sup> handling [43], we investigated ROS production and Ca<sup>2+</sup> handling in isolated adult rat CMs exposed to 5 μM heme for 6 h. In agreement with data on pro-oxidant effects of heme in neonatal mouse CMs (Figure 1D-F), oxidative stress was significantly increased in adult rat CMs exposed to free heme (see Figure 1 in [37]). Accordingly, heme-treated adult CMs had significantly reduced systolic Ca<sup>2+</sup> transient amplitudes (by 37%, Figure 4A-C) in the face of slowed relaxation kinetics, indicating reduced SR Ca<sup>2+</sup> re-uptake upon heme exposure (Figure 4D). In line with this, fractional shortening of isolated heme-treated CMs was significantly reduced as compared to vehicle-treated CMs (Figure 4E). Vice versa, ROS-scavenging by the use of NAC (10 mM) attenuated heme-dependent Ca<sup>2+</sup>-mishandling and largely preserved single cell contractility (Figure 4A-E). As well as NAC, Hx co-treatment significantly improved systolic Ca<sup>2+</sup> transients and accelerated Ca<sup>2+</sup> transient decay kinetics, which resulted in a significant improvement of cardiomyocyte contractility (Figure 4A-E).

In keeping with these Ca<sup>2+</sup> handling alterations, Hx<sup>-/-</sup> hearts displayed a higher amount of oxidized ryanodine receptor 2 (RYR2) than wild-type controls (Figure 5A), which may have further contributed to disturbed SR Ca handling on top of decreased SR Ca<sup>2+</sup> reuptake, which was evidenced by slower kinetics of diastolic Ca<sup>2+</sup> decay. Furthermore, Hx<sup>-/-</sup> hearts showed a more pronounced oxidation of the intracellular stress kinase Ca<sup>2+</sup>/Calmodulin-dependent protein kinase II (CaMKII) (Figure 5B). Consistently, CaMKII-dependent phosphorylation of RyR2 (Ser-2814) and Phospholamban (PLB) (Thr-17) were significantly higher in Hx<sup>-/-</sup> hearts than in wild-type controls (Figure 5C, D).

Altogether, these data unravel a key role for Hx in preventing systolic dysfunction related to heme-driven oxidative stress and Ca<sup>2+</sup> mishandling.

**Hemopexin cardioprotective effect is mediated by its anti-oxidant properties**

Our data demonstrate that free heme accumulating in the heart when Hx is lost promotes systolic dysfunction. Moreover, our *in vitro* results suggest that Hx is protective because it limits heme-driven oxidative stress, as well as the anti-oxidant NAC. To confirm these data *in vivo*, we performed rescue experiments in hemolytic mice treated with either Hx or the anti-oxidant agent  $\alpha$ -tocopherol.

Wild-type mice were treated with PHZ and Hx,  $\alpha$ -tocopherol or vehicle for 4 weeks. As expected,  $\alpha$ -tocopherol treatment prevented ROS accumulation and the induction of anti-oxidant genes in the heart (Figure 6A, B and see Figure 8 in [37]). Hx treatment similarly prevented heme accumulation within the heart as demonstrated by the blunted induction of HO-1 in Hx-treated hemolytic mice, and normalised anti-oxidant gene expression profile (Figure 6C, D). Importantly, when mice were treated with PHZ together with either Hx or  $\alpha$ -tocopherol, systolic function was preserved (Figure 6E-J).

We conclude that Hx is cardioprotective because it limits heme-driven oxidative damage.

**Discussion**

Here, we show that Hx preserves systolic function by preventing heme-driven ROS accumulation in cardiomyocytes and the ensuing perturbation of  $\text{Ca}^{2+}$  handling (Figure 7). This has potentially important implications for patients suffering from pathologic conditions associated with free heme and heme overload, such as hemolytic anemias and hemoglobinopathies.

Data obtained in  $\text{Hx}^{-/-}$  mice indicate that Hx has a key homeostatic role in preserving ventricular function under steady-state, when the physiological rate of hemolysis is very low and is well-controlled by physiologic systems such as Hx or haptoglobin [44]. Although a role for pathologic free iron (non-transferrin bound iron, NTBI) has been suggested in non-transfusion-dependent and

transfusion-dependent hemolytic anemias [45, 46], our data highlight a novel concept that heart might be susceptible to acute exposure to free heme (non-hemopexin bound heme, NHBH), and that Hx critically maintains cardiomyocyte function by scavenging free heme and avoiding cell heme overload (Figure 7). The specific uptake of Hx-heme complexes by the liver ultimately allows safe terminal heme detoxification [19].

Notably, the cardioprotective role of Hx can be even more critical in circumstances of chronic hemolysis as occurs in hemolytic disorders when huge amount of hemoglobin is released into the bloodstream. It has been shown that free hemoglobin affects heart function in rabbits and exacerbates cardiotoxicity of LPS in experimental models of sepsis [47-49]. The heme moiety of hemoglobin, which is released following hemoglobin oxidation in the pro-oxidant plasma milieu, is thought to mediate hemoglobin toxicity [50]. Our finding that Hx prevents systolic dysfunction in an experimental model of intravascular hemolysis, such as in PHZ-treated mice, supports this view and conclusively proves a causative role for NHBH in left ventricular dysfunction associated to hemolytic disorders. Furthermore, Hx could be important in case of cardiac valve surgery, where mechanical forces and shear stress are significantly increased [51, 52]. Consistently, hemolysis associated to high shear stress has been reported after mitral valve repair [51, 52] and could contribute to heart failure in these patients.

Finally, we can speculate that Hx is beneficial during cardiac infarction, when myoglobin is released from injured cardiomyocytes. Once liberated from muscle cells, myoglobin rapidly auto-oxidizes, which in turn promotes the spontaneous loss of hemin [53-56] that might contribute to the establishment of oxidative stress and systolic dysfunction.

Heme is a strong driver of oxidation since iron can participate in the Fenton reaction for producing the hydroxyl radical. As a hydrophobic molecule, heme intercalates into lipid membranes promoting

lipid peroxidation, both at the plasma membrane and in subcellular compartments [8, 13] [17]. Consistently, we measured increased lipid peroxidation in both cells and tissues exposed to free heme, which can be rescued by  $\alpha$ -tocopherol, an agent able to react with lipid radicals and interrupt the oxidation reaction. Mechanistically, heme-derived ROS may directly modify  $\text{Ca}^{2+}$  handling proteins (such as the RyR2 or SERCA2a) [35, 57], and may also activate intracellular stress kinases, such as CaMKII [58], which in turn phosphorylate the same  $\text{Ca}^{2+}$  effectors and ultimately exacerbate  $\text{Ca}^{2+}$  mishandling. In agreement, heme has been previously reported to promote oxidation of myofilament proteins, including filamin C, myosin heavy chain, cardiac myosin binding protein C, and  $\alpha$ -actinin in human cardiomyocytes [16].

Our data further extend this view and indicate that free heme triggers oxidation of major regulators of  $\text{Ca}^{2+}$  trafficking, such as RyR2, *in vivo*. Furthermore, oxidatively activated CaMKII was increased in Hx<sup>-/-</sup> hearts and was paralleled by CaMKII-specific hyperphosphorylation of RyR2 and PLB. Altogether, these modifications of  $\text{Ca}^{2+}$  effectors were associated with impaired intracellular  $\text{Ca}^{2+}$  handling, resulting in decreased single cell contractility, which points to disrupted  $\text{Ca}^{2+}$  handling in cardiac myocytes as a major mechanism underlying the impaired cardiac function of Hx<sup>-/-</sup> mice. In particular, the finding that  $\text{Ca}^{2+}$  transient decay kinetics, as an approximation of SR  $\text{Ca}^{2+}$  reuptake, were significantly slower in the absence of Hx, suggests that the *direct* effects of ROS on SERCA2a/PLB function overcome CaMKII-dependent effects on PLB, which would instead lead to accelerated SR  $\text{Ca}^{2+}$  reuptake. On the other hand, CaMKII-dependent regulation of RyR2 and heme-induced oxidation of RyR2 both contribute to diastolic SR  $\text{Ca}^{2+}$  leakage and SR  $\text{Ca}^{2+}$  depletion and tend to decrease SR  $\text{Ca}^{2+}$  stores. Intriguingly, treatment with Hx or NAC preserves intracellular  $\text{Ca}^{2+}$  handling and single cell contractility and thus further supports a model where direct heme/ROS-mediated effects on  $\text{Ca}^{2+}$  handling proteins is the main cause of reduced cardiac function when Hx is depleted.

Intriguingly, intracellular heme can trigger oxidative modification of the mitochondrial outer membrane voltage-dependent anion channel (VDAC) [59], thus impairing mitochondrial  $\text{Ca}^{2+}$  influx [60]. This has been uncovered in endothelial cells and a similar mechanism is likely to occur in cardiomyocytes. Given the close juxtaposition of SR RyR  $\text{Ca}^{2+}$  channels and mitochondrial calcium transporters [61], alterations in sarcoplasmic  $\text{Ca}^{2+}$  homeostasis are expected to further amplify mitochondrial ROS generation [62], exacerbating the pro-oxidant cardiomyocyte status.

It is of note that SR  $\text{Ca}^{2+}$  leakage resulting from either hyper-phosphorylation or oxidation of RyR2 is a major determinant of ventricular arrhythmias [43, 63] and these electrical abnormalities also represent one of the most severe complications in patients carrying mechanical circulatory support devices, a condition in which the heart is subjected to high shear stress [64]. Our data showing RyR2 alterations and  $\text{Ca}^{2+}$  mishandling in heme-exposed cardiomyocytes thus suggest that heme might display a pro-arrhythmogenic effect. This is of particular interest in the context of non-transfusion dependent  $\beta$ -thalassemic syndromes, largely complicated by heart failure and severe arrhythmias [65-67].

Altogether, our findings have important implications for the treatment of pathologic conditions associated with heme overload. In fact, heart disease is the primary determinant of prognosis and survival in hemolytic disorders [18, 68]. In  $\beta$ -thalassemia patients, cardiac complications represent the primary cause of mortality and one of the major causes of morbidity [18, 68]. In these patients, heart failure is the result of impaired left systolic function and ventricular dilatation, resulting from multiple factors [18]. Among them, NTBI has been recently recognized as initiating factor of cardiomyopathy in  $\beta$ -thalassemic patients [45, 46, 69]. NTBI results from multiple blood transfusions and increased iron absorption associated with ineffective erythropoiesis, and it is cleared preferentially by the liver and the myocardium, at a rate exceeding 200 times that of transferrin-bound iron [45, 70]. In the heart, NTBI catalyzes the formation of free radicals, resulting

in oxidative stress that eventually contributes to organ dysfunction. Here, we propose NHBH as new and additional factor participating to left ventricular dysfunction in  $\beta$ -thalassemia. Indeed, our data in  $\beta$ -thalassemic mice highlight an association between Hx depletion/heme overload in the heart and systolic dysfunction, suggesting that the sequestration of NHBH by exogenous Hx might provide further benefits in limiting free-heme related organ damage. We can speculate that a combined therapy with iron and heme chelators would be beneficial in counteracting cardiac damage induced by NTBI and NHBH. Collectively, our data support the use of Hx as a therapeutic option to prevent/limit heme-driven cytotoxicity in heme-overload conditions.

### **Funding**

This work was supported by Telethon Grant GGP12082 to E.T.

### **Acknowledgments**

We thank Nathan Brinkman (CSL Behring) for supply of hemopexin. We are grateful to Alessandro Mattè (Dept. of Medicine, Università degli Studi di Verona–Azienda Ospedaliera Universitaria Integrata Verona, Verona, Italy) for  $\beta$ -thalassemic mice breeding.

### **Author Disclosure Statement**

ET has received research funding from CSL Behring.

## References

- [1] T. Oka, I. Komuro, Molecular mechanisms underlying the transition of cardiac hypertrophy to heart failure, *Circ J* 72 Suppl A (2008) A13-6.
- [2] M.P. Sumandea, S.F. Steinberg, Redox signaling and cardiac sarcomeres, *J Biol Chem* 286(12) (2011) 9921-7.
- [3] H. Tsutsui, S. Kinugawa, S. Matsushima, Oxidative stress and heart failure, *Am J Physiol Heart Circ Physiol* 301(6) (2011) H2181-90.
- [4] M.T. Gladwin, V. Sachdev, Cardiovascular abnormalities in sickle cell disease, *J Am Coll Cardiol* 59(13) (2012) 1123-33.
- [5] V. Sachdev, R.F. Machado, Y. Shizukuda, Y.N. Rao, S. Sidenko, I. Ernst, M. St Peter, W.A. Coles, D.R. Rosing, W.C. Blackwelder, O. Castro, G.J. Kato, M.T. Gladwin, Diastolic dysfunction is an independent risk factor for death in patients with sickle cell disease, *J Am Coll Cardiol* 49(4) (2007) 472-9.
- [6] D.J. Hausenloy, D.M. Yellon, Myocardial ischemia-reperfusion injury: a neglected therapeutic target, *J Clin Invest* 123(1) (2013) 92-100.
- [7] N. Hamdani, V. Kooij, S. van Dijk, D. Merkus, W.J. Paulus, C.D. Remedios, D.J. Duncker, G.J. Stienen, J. van der Velden, Sarcomeric dysfunction in heart failure, *Cardiovasc Res* 77(4) (2008) 649-58.
- [8] K.T. Sawicki, H.C. Chang, H. Ardehali, Role of heme in cardiovascular physiology and disease, *J Am Heart Assoc* 4(1) (2015) e001138.
- [9] F. Vinchi, L. De Franceschi, A. Ghigo, T. Townes, J. Cimino, L. Silengo, E. Hirsch, F. Altruda, E. Tolosano, Hemopexin therapy improves cardiovascular function by preventing heme-induced endothelial toxicity in mouse models of hemolytic diseases, *Circulation* 127(12) (2013) 1317-29.
- [10] G. Balla, G.M. Vercellotti, U. Muller-Eberhard, J. Eaton, H.S. Jacob, Exposure of endothelial cells to free heme potentiates damage mediated by granulocytes and toxic oxygen species, *Lab Invest* 64(5) (1991) 648-55.
- [11] G. Balla, H.S. Jacob, J.W. Eaton, J.D. Belcher, G.M. Vercellotti, Hemin: a possible physiological mediator of low density lipoprotein oxidation and endothelial injury, *Arterioscler Thromb* 11(6) (1991) 1700-11.
- [12] J. Balla, H.S. Jacob, G. Balla, K. Nath, J.W. Eaton, G.M. Vercellotti, Endothelial-cell heme uptake from heme proteins: induction of sensitization and desensitization to oxidant damage, *Proc Natl Acad Sci U S A* 90(20) (1993) 9285-9.
- [13] V. Jeney, J. Balla, A. Yachie, Z. Varga, G.M. Vercellotti, J.W. Eaton, G. Balla, Pro-oxidant and cytotoxic effects of circulating heme, *Blood* 100(3) (2002) 879-87.
- [14] J.W. Deuel, F. Vallelian, C.A. Schaer, M. Puglia, P.W. Buehler, D.J. Schaer, Different target specificities of haptoglobin and hemopexin define a sequential protection system against vascular hemoglobin toxicity, *Free Radic Biol Med* 89 (2015) 931-43.
- [15] R.N. Hasan, A.I. Schafer, Hemin upregulates Egr-1 expression in vascular smooth muscle cells via reactive oxygen species ERK-1/2-Elk-1 and NF-kappaB, *Circ Res* 102(1) (2008) 42-50.
- [16] G. Alvarado, V. Jeney, A. Tóth, É. Csósz, G. Kalló, A.T. Huynh, C. Hajnal, J. Kalász, E.T. Pásztor, I. Édes, M. Gram, B. Akerström, A. Smith, J.W. Eaton, G. Balla, Z. Papp, J. Balla, Heme-induced contractile dysfunction in Human cardiomyocytes caused by oxidant damage to thick filament proteins, *Free Radic Biol Med* 89 (2015) 248-262.
- [17] D. Chiabrando, F. Vinchi, V. Fiorito, S. Mercurio, E. Tolosano, Heme in pathophysiology: a matter of scavenging, metabolism and trafficking across cell membranes, *Front Pharmacol* 5 (2014) 61.
- [18] D.T. Kremastinos, D. Farmakis, A. Aessopos, G. Hahalis, E. Hamodraka, D. Tsiapras, A. Keren, beta-Thalassemia Cardiomyopathy History, Present Considerations, and Future Perspectives, *Circulation-Heart Failure* 3(3) (2010) 451-458.
- [19] E. Tolosano, S. Fagoonee, N. Morello, F. Vinchi, V. Fiorito, Heme scavenging and the other facets of hemopexin, *Antioxid Redox Signal* 12(2) (2010) 305-20.
- [20] F. Vinchi, S. Gastaldi, L. Silengo, F. Altruda, E. Tolosano, Hemopexin prevents endothelial damage and liver congestion in a mouse model of heme overload, *Am J Pathol* 173(1) (2008) 289-99.
- [21] F. Vinchi, E. Tolosano, Therapeutic approaches to limit hemolysis-driven endothelial dysfunction: scavenging free heme to preserve vasculature homeostasis, *Oxid Med Cell Longev* 2013 (2013) 396527.

- [22] S. Rolla, G. Ingoglia, V. Bardina, L. Silengo, F. Altruda, F. Novelli, E. Tolosano, Acute-phase protein hemopexin is a negative regulator of Th17 response and experimental autoimmune encephalomyelitis development, *J Immunol* 191(11) (2013) 5451-9.
- [23] J.D. Belcher, C. Chen, J. Nguyen, L. Milbauer, F. Abdulla, A.I. Alayash, A. Smith, K.A. Nath, R.P. Hebbel, G.M. Vercellotti, Heme triggers TLR4 signaling leading to endothelial cell activation and vaso-occlusion in murine sickle cell disease, *Blood* 123(3) (2014) 377-90.
- [24] S. Ghosh, O.A. Adisa, P. Chappa, F. Tan, K.A. Jackson, D.R. Archer, S.F. Ofori-Acquah, Extracellular heme crisis triggers acute chest syndrome in sickle mice, *J Clin Invest* 123(11) (2013) 4809-20.
- [25] E. Tolosano, E. Hirsch, E. Patrucco, C. Camaschella, R. Navone, L. Silengo, F. Altruda, Defective recovery and severe renal damage after acute hemolysis in hemopexin-deficient mice, *Blood* 94(11) (1999) 3906-14.
- [26] V. Fiorito, S. Geninatti Crich, L. Silengo, S. Aime, F. Altruda, E. Tolosano, Lack of Plasma Protein Hemopexin Results in Increased Duodenal Iron Uptake, *PLoS One* 8(6) (2013) e68146.
- [27] S.S. Franco, L. De Falco, S. Ghaffari, C. Brugnara, D.A. Sinclair, A. Matte', A. Iolascon, N. Mohandas, M. Bertoldi, X. An, A. Siciliano, P. Rimmelé, M.D. Cappellini, S. Michan, E. Zoratti, J. Anne, L. De Franceschi, Resveratrol accelerates erythroid maturation by activation of FoxO3 and ameliorates anemia in beta-thalassemic mice, *Haematologica* 99(2) (2014) 267-75.
- [28] A. Matte, M. Bertoldi, N. Mohandas, X. An, A. Bugatti, A.M. Brunati, M. Rusnati, E. Tibaldi, A. Siciliano, F. Turrini, S. Perrotta, L. De Franceschi, Membrane association of peroxiredoxin-2 in red cells is mediated by the N-terminal cytoplasmic domain of band 3, *Free Radic Biol Med* 55 (2013) 27-35.
- [29] A. Matte, L. De Falco, A. Iolascon, N. Mohandas, X. An, A. Siciliano, C. Leboeuf, A. Janin, M. Bruno, S.Y. Choi, D.W. Kim, L. De Franceschi, The Interplay Between Peroxiredoxin-2 and Nuclear Factor-Erythroid 2 Is Important in Limiting Oxidative Mediated Dysfunction in  $\beta$ -Thalassemic Erythropoiesis, *Antioxid Redox Signal* 23(16) (2015) 1284-97.
- [30] S. Sassa, Sequential induction of heme pathway enzymes during erythroid differentiation of mouse Friend leukemia virus-infected cells, *J Exp Med* 143(2) (1976) 305-15.
- [31] D. Chiabrando, S. Marro, S. Mercurio, C. Giorgi, S. Petrillo, F. Vinchi, V. Fiorito, S. Fagoonee, A. Camporeale, E. Turco, G.R. Merlo, L. Silengo, F. Altruda, P. Pinton, E. Tolosano, The mitochondrial heme exporter FLVCR1b mediates erythroid differentiation, *J Clin Invest* 122(12) (2012) 4569-79.
- [32] V. Fiorito, M. Forni, L. Silengo, F. Altruda, E. Tolosano, Crucial Role of FLVCR1a in the Maintenance of Intestinal Heme Homeostasis, *Antioxid Redox Signal* 23(18) (2015) 1410-23.
- [33] C.M. Sag, H.A. Wolff, K. Neumann, M.K. Opiela, J. Zhang, F. Steuer, T. Sowa, S. Gupta, M. Schirmer, M. Hünlich, M. Rave-Fränk, C.F. Hess, M.E. Anderson, A.M. Shah, H. Christiansen, L.S. Maier, Ionizing radiation regulates cardiac Ca handling via increased ROS and activated CaMKII, *Basic Res Cardiol* 108(6) (2013) 385.
- [34] H. Puchtler, F.S. Waldrop, L.S. Valentine, Polarization microscopic studies of connective tissue stained with picro-sirius red FBA, *Beitr Pathol* 150(2) (1973) 174-87.
- [35] C.M. Sag, A.C. Köhler, M.E. Anderson, J. Backs, L.S. Maier, CaMKII-dependent SR Ca leak contributes to doxorubicin-induced impaired Ca handling in isolated cardiac myocytes, *J Mol Cell Cardiol* 51(5) (2011) 749-59.
- [36] F. Vinchi, M. Costa da Silva, G. Ingoglia, S. Petrillo, N. Brinkman, A. Zuercher, A. Cerwenka, E. Tolosano, M.U. Muckenthaler, Hemopexin therapy reverts heme-induced proinflammatory phenotypic switching of macrophages in a mouse model of sickle cell disease, *Blood* 127(4) (2016) 473-86.
- [37] G. Ingoglia, C.M. Sag, N. Rex, L. De Franceschi, F. Vinchi, J. Cimino, S. Petrillo, S. Wagner, K. Kreitmeier, L. Silengo, F. Altruda, L.S. Maier, E. Hirsch, A. Ghigo, E. Tolosano, Hemopexin limits heme accumulation and oxidative stress in cardiac cells, *Data in Brief, submitted* Data in Brief, submitted (2017).
- [38] S. Mercurio, S. Petrillo, D. Chiabrando, Z.I. Bassi, D. Gays, A. Camporeale, A. Vacaru, B. Miniscalco, G. Valperga, L. Silengo, F. Altruda, M.H. Baron, M.M. Santoro, E. Tolosano, The heme exporter Flvcr1 regulates expansion and differentiation of committed erythroid progenitors by controlling intracellular heme accumulation, *Haematologica* 100(6) (2015) 720-9.
- [39] F. Vinchi, G. Ingoglia, D. Chiabrando, S. Mercurio, E. Turco, L. Silengo, F. Altruda, E. Tolosano, Heme exporter FLVCR1a regulates heme synthesis and degradation and controls activity of cytochromes P450, *Gastroenterology* 146(5) (2014) 1325-38.



- [40] Z. Cao, H. Zhu, L. Zhang, X. Zhao, J.L. Zweier, Y. Li, Antioxidants and phase 2 enzymes in cardiomyocytes: Chemical inducibility and chemoprotection against oxidant and simulated ischemia-reperfusion injury, *Exp Biol Med (Maywood)* 231(8) (2006) 1353-64.
- [41] H. Zhu, Z. Jia, B.R. Misra, L. Zhang, Z. Cao, M. Yamamoto, M.A. Trush, H.P. Misra, Y. Li, Nuclear factor E2-related factor 2-dependent myocardial cytoprotection against oxidative and electrophilic stress, *Cardiovasc Toxicol* 8(2) (2008) 71-85.
- [42] L. De Franceschi, F. Daraio, A. Filippini, S. Carturan, E.M. Muchitsch, A. Roetto, C. Camaschella, Liver expression of hepcidin and other iron genes in two mouse models of beta-thalassemia, *Haematologica* 91(10) (2006) 1336-42.
- [43] C.M. Sag, S. Wagner, L.S. Maier, Role of oxidants on calcium and sodium movement in healthy and diseased cardiac myocytes, *Free Radic Biol Med* 63 (2013) 338-49.
- [44] D.J. Schaer, F. Vinchi, G. Ingoglia, E. Tolosano, P.W. Buehler, Haptoglobin, hemopexin, and related defense pathways-basic science, clinical perspectives, and drug development, *Front Physiol* 5 (2014) 415.
- [45] A. Piga, F. Longo, L. Duca, S. Roggero, T. Vinciguerra, R. Calabrese, C. Hershko, M.D. Cappellini, High nontransferrin bound iron levels and heart disease in thalassemia major, *Am J Hematol* 84(1) (2009) 29-33.
- [46] K. Wijarnpreecha, N. Siri-Angkul, K. Shinlapawittayatorn, P. Charoenkwan, S. Silvilairat, C. Siwasomboon, P. Visarutratna, S. Srichairatanakool, A. Tantiworawit, A. Phrommintikul, S.C. Chattipakorn, N. Chattipakorn, Heart Rate Variability as an Alternative Indicator for Identifying Cardiac Iron Status in Non-Transfusion Dependent Thalassemia Patients, *PLoS One* 10(6) (2015) e0130837.
- [47] C. Krishnamurti, A.J. Carter, P. Maglasang, J.R. Hess, M.A. Cutting, B.M. Alving, Cardiovascular toxicity of human cross-linked hemoglobin in a rabbit endotoxemia model, *Crit Care Med* 25(11) (1997) 1874-80.
- [48] J.H. Baek, X. Zhang, M.C. Williams, D.J. Schaer, P.W. Buehler, F. D'Agnillo, Extracellular Hb enhances cardiac toxicity in endotoxemic guinea pigs: protective role of haptoglobin, *Toxins (Basel)* 6(4) (2014) 1244-59.
- [49] S. Nemeto, M. Aoki, C. Dehua, Y. Imai, Free hemoglobin impairs cardiac function in neonatal rabbit hearts, *Ann Thorac Surg* 69(5) (2000) 1484-9.
- [50] D.J. Schaer, P.W. Buehler, A.I. Alayash, J.D. Belcher, G.M. Vercellotti, Hemolysis and free hemoglobin revisited: exploring hemoglobin and hemin scavengers as a novel class of therapeutic proteins, *Blood* 121(8) (2013) 1276-84.
- [51] D. Acharya, D.C. McGiffin, Hemolysis after mitral valve repair, *J Card Surg* 28(2) (2013) 129-32.
- [52] T.C. Yeo, W.K. Freeman, H.V. Schaff, T.A. Orszulak, Mechanisms of hemolysis after mitral valve repair: assessment by serial echocardiography, *J Am Coll Cardiol* 32(3) (1998) 717-23.
- [53] J.C. Mocny, J.S. Olson, T.D. Connell, Passively released heme from hemoglobin and myoglobin is a potential source of nutrient iron for *Bordetella bronchiseptica*, *Infect Immun* 75(10) (2007) 4857-66.
- [54] M.S. Hargrove, E.W. Singleton, M.L. Quillin, L.A. Ortiz, G.N. Phillips, J.S. Olson, A.J. Mathews, His64(E7)->Tyr apomyoglobin as a reagent for measuring rates of hemin dissociation, *J Biol Chem* 269(6) (1994) 4207-14.
- [55] M.S. Hargrove, D. Barrick, J.S. Olson, The association rate constant for heme binding to globin is independent of protein structure, *Biochemistry* 35(35) (1996) 11293-9.
- [56] M.S. Hargrove, J.S. Olson, The stability of holomyoglobin is determined by heme affinity, *Biochemistry* 35(35) (1996) 11310-8.
- [57] A.C. Köhler, C.M. Sag, L.S. Maier, Reactive oxygen species and excitation-contraction coupling in the context of cardiac pathology, *J Mol Cell Cardiol* 73 (2014) 92-102.
- [58] J.R. Erickson, M.L. Joiner, X. Guan, W. Kutschke, J. Yang, C.V. Oddis, R.K. Bartlett, J.S. Lowe, S.E. O'Donnell, N. Aykin-Burns, M.C. Zimmerman, K. Zimmerman, A.J. Ham, R.M. Weiss, D.R. Spitz, M.A. Shea, R.J. Colbran, P.J. Mohler, M.E. Anderson, A dynamic pathway for calcium-independent activation of CaMKII by methionine oxidation, *Cell* 133(3) (2008) 462-74.
- [59] A.N. Higdon, G.A. Benavides, B.K. Chacko, X. Ouyang, M.S. Johnson, A. Landar, J. Zhang, V.M. Darley-Usmar, Hemin causes mitochondrial dysfunction in endothelial cells through promoting lipid peroxidation: the protective role of autophagy, *Am J Physiol Heart Circ Physiol* 302(7) (2012) H1394-409.

- [60] D. Gincel, H. Zaid, V. Shoshan-Barmatz, Calcium binding and translocation by the voltage-dependent anion channel: a possible regulatory mechanism in mitochondrial function, *Biochem J* 358(Pt 1) (2001) 147-55.
- [61] G. Szalai, G. Csordás, B.M. Hantash, A.P. Thomas, G. Hajnóczy, Calcium signal transmission between ryanodine receptors and mitochondria, *J Biol Chem* 275(20) (2000) 15305-13.
- [62] P.S. Brookes, Y. Yoon, J.L. Robotham, M.W. Anders, S.S. Sheu, Calcium, ATP, and ROS: a mitochondrial love-hate triangle, *Am J Physiol Cell Physiol* 287(4) (2004) C817-33.
- [63] P.D. Swaminathan, A. Purohit, T.J. Hund, M.E. Anderson, Calmodulin-dependent protein kinase II: linking heart failure and arrhythmias, *Circ Res* 110(12) (2012) 1661-77.
- [64] H. Patel, R. Madanieh, C.E. Kosmas, S.K. Vatti, T.J. Vittorio, Complications of Continuous-Flow Mechanical Circulatory Support Devices, *Clin Med Insights Cardiol* 9(Suppl 2) (2015) 15-21.
- [65] M.D. Cappellini, J.B. Porter, K.M. Musallam, A. Kattamis, V. Viprakasit, R. Galanello, A.T. Taher, Development of a new disease severity scoring system for patients with non-transfusion-dependent thalassemia, *Eur J Intern Med* 28 (2016) 91-6.
- [66] A.T. Taher, K.M. Musallam, A.N. Saliba, G. Graziadei, G. Garziadei, M.D. Cappellini, Hemoglobin level and morbidity in non-transfusion-dependent thalassemia, *Blood Cells Mol Dis* 55(2) (2015) 108-9.
- [67] A.T. Taher, M.D. Cappellini, Y. Aydinok, J.B. Porter, Z. Karakas, V. Viprakasit, N. Siritanaratkul, A. Kattamis, C. Wang, Z. Zhu, V. Joaquin, M.J. Uwamahoro, Y.R. Lai, Optimising iron chelation therapy with deferasirox for non-transfusion-dependent thalassaemia patients: 1-year results from the THETIS study, *Blood Cells Mol Dis* 57 (2016) 23-9.
- [68] E.A. Rachmilewitz, P.J. Giardina, How I treat thalassemia, *Blood* 118(13) (2011) 3479-88.
- [69] A. Roghi, E. Poggiali, L. Duca, A. Mafrici, P. Pedrotti, S. Paccagnini, S. Brenna, A. Galli, D. Consonni, M.D. Cappellini, Role of Non-Transferrin-Bound Iron in the pathogenesis of cardiotoxicity in patients with ST-elevation myocardial infarction assessed by Cardiac Magnetic Resonance Imaging, *Int J Cardiol* 199 (2015) 326-32.
- [70] C. Hershko, Pathogenesis and management of iron toxicity in thalassemia, *Ann N Y Acad Sci* 1202 (2010) 1-9.

**Tables****Table 1. Echocardiographic parameters of Wt and Hx<sup>-/-</sup> mice.**

<b>ECHOCARDIOGRAPHY</b>	<b>Wt</b>	<b>Hx<sup>-/-</sup></b>	<b>t-test</b>
Left ventricle internal dimension (diastole) (mm)	3,35 ± 0,25	3,65 ± 0,27	NS
Left ventricle internal dimension (systole) (mm)	1,84 ± 0,07	2,42 ± 0,27	P ≤ 0.01
Intraventricular septum (diastole) (mm)	0,79 ± 0,09	0,79 ± 0,04	NS
Intraventricular septum (systole) (mm)	1,25 ± 0,13	1,24 ± 0,06	NS
Left posterior wall (diastole) (mm)	0,74 ± 0,08	0,82 ± 0,06	NS
Left posterior wall (systole) (mm)	1,13 ± 0,11	1,21 ± 0,06	NS
Hypertrophic index	0,83 ± 0,13	0,97 ± 0,07	NS
Left ventricle mass (mg)	70,26 ± 11,52	79,69 ± 13,56	NS

**Table 2. Echocardiographic parameters of Wt and β-thalassemic (β-Thal) mice.**

<b>ECHOCARDIOGRAPHY</b>	<b>Wt</b>	<b>β -Thal</b>	<b>t-test</b>
Left ventricle internal dimension (diastole) (mm)	4,09 ± 0,32	4,60 ± 0,35	NS
Left ventricle internal dimension (systole) (mm)	2,59 ± 0,22	3,28 ± 0,32	P < 0.05
Intraventricular septum (diastole) (mm)	0,66 ± 0,12	0,77 ± 0,08	NS
Intraventricular septum (systole) (mm)	1,22 ± 0,14	1,24 ± 0,12	NS
Left posterior wall (diastole) (mm)	0,77 ± 0,10	0,80 ± 0,08	NS
Left posterior wall (systole) (mm)	1,21 ± 0,21	1,15 ± 0,16	NS
Hypertrophic index	0,98 ± 0,16	1,41 ± 0,08	P < 0.05
Left ventricle mass (mg)	86,29 ± 27,07	116,65 ± 23	NS

## Figure legends

**Figure 1. Hemopexin protects neonatal cardiomyocytes from heme accumulation and ROS production.** Data on neonatal cardiomyocytes isolated from the hearts of postnatal day 0-1 wild-type (Wt) pups, untreated (NT) or treated with 10  $\mu$ M Hx-heme complex, 10  $\mu$ M Albumin (Alb)-heme complex or 10  $\mu$ M heme for 8 hours, are shown. (A) Cardiomyocyte heme content. (B) qRT-PCR analysis of Ho-1 mRNA levels. (C) Western blot analysis of HO-1. (D) Cardiomyocyte ROS content and (E) immunofluorescence analysis of super-oxide radical formation (super-oxide radical was stained with Mito-sox fluorescent probe. Nuclei were stained with DAPI). (F) qRT-PCR analysis of Gsr mRNA levels. Results shown are representative of three independent experiments. One-way analysis of variance with Bonferroni post-test analysis was performed. \*P < 0.05; \*\*P < 0.01; \*\*\*P < 0.001. Values represent mean  $\pm$  SEM. AU, arbitrary units; RQ, relative quantity; FIU, fluorescence intensity unit.

**Figure 2. Hemopexin prevents heme-driven cardiac oxidative stress.** Data on the heart of Wt and Hx<sup>-/-</sup> mice are shown. (A) Heme content (n=5). (B) qRT-PCR, representative western blot and immunohistochemistry analysis for HO-1. (C) ROS content (n=13) and (D) malondialdehyde (MDA; n=8) content. (E) qRT-PCR analysis of Gsr mRNA levels. In Western blot shown in B, each lane represents an individual animal; Bip was used as loading control. Unpaired t-test analysis with Welch's correction was performed. Values represent mean  $\pm$  SEM. \*P<0.05.

**Figure 3. Hemopexin prevents heme overload-induced heart dysfunction.** Data on the heart of Wt and Hx<sup>-/-</sup> mice (A-C), Wt and  $\beta$ -thalassemic ( $\beta$ -Thal) mice (D-F) and PHZ-treated Wt mice (G-I) are shown. (A) Representative M-mode echocardiogram of a Wt and an Hx<sup>-/-</sup> mouse. (B) Fractional shortening and (C) ejection fraction at 3 (Wt n=10; Hx<sup>-/-</sup> n=20) and 6 (Wt n=5; Hx<sup>-/-</sup> n=3) months of age. (D) Representative M-mode echocardiogram of a Wt and a  $\beta$ -thalassemic mouse. (E) Fractional shortening and (F) ejection fraction (Wt n=3;  $\beta$ -Thal n=6). (G) Representative M-mode

echocardiogram of a Wt mouse at time 0 and after 4 weeks of PHZ treatment. (H) Fractional shortening and (I) ejection fraction (n=10). Two-ways analysis of variance with Bonferroni post-test analysis (B-C) and unpaired t-test analysis with Welch's correction (E-F, H-I) were performed. \*P < 0.05; \*\*P < 0.01; \*\*\*P < 0.001. Values represent mean  $\pm$  SEM.

**Figure 4. Hemopexin prevents heme-induced Ca<sup>2+</sup> mishandling.** Data on isolated adult rat CMs exposed to heme (5  $\mu$ M), Hx-heme (5  $\mu$ M), NAC-heme (10 mM) or vehicle (Nt) are shown. Representative calcium transients (A), and representative single cell contractility (B) of untreated, heme-treated, Hx-heme-treated and NAC-heme-treated CMs. Bar graphs represent (C) systolic calcium transient amplitude, as the difference of peak amplitude of the fluorescence ( $\Delta$ F<sub>340/380</sub> = F<sub>340/380</sub> peak – F<sub>340/380</sub> basal), (D) relaxation kinetics as Ca<sup>2+</sup> decay and (E) contractility of untreated (n = 37) heme-treated (n = 103), heme-Hx-treated (n = 91) and heme-NAC-treated (n= 22) CMs. t-test analysis with Welch's correction was performed. \*P < 0.05. Values represent mean  $\pm$  SEM.

**Figure 5. Hemopexin prevents oxidative alteration of Ca<sup>2+</sup> handling proteins.** Data on the heart of Wt and Hx<sup>-/-</sup> mice are shown. (A) Immunoprecipitation of oxidized RyR2. RyR2 was immunoprecipitated with a specific antibody and blotted with either oxyblot or the specific antibody. (B) Western blot analysis of  $\alpha$  and  $\beta$  oxidized CaMKII and total CaMKII.  $\alpha$  and  $\beta$  oxidized CaMKII were normalized on total CaMKII. Western blot analysis of (C) phosphorylated RyR 2 at serine 2814 (RyR2 pSer2814) normalized on total RyR2, and (D) phosphorylated PLB at threonine 17 (PLB pThr17) normalized on total PLB. A representative blot of at least 3 independent experiments is shown. For densitometry analyses on the right, n=5 for each genotype. In B-D, Total CaMKII, RyR2 and PLB are normalized on vinculin, used as a loading control. Unpaired t-test analysis with Welch's correction was performed. \*P < 0.05; \*\*P < 0.01. Values represent mean  $\pm$  SEM.

**Figure 6. Hemopexin protective effects are mediated by its anti-oxidant properties**

Data on the heart of PHZ-treated Wt mice administered or not with  $\alpha$ -tocopherol or Hx are shown. (A) ROS content and (B) qRT-PCR analysis of Thioredoxin Red and Gsr mRNA levels in untreated (n=12), PHZ- (n=8) and PHZ- $\alpha$ -tocopherol-treated Wt mice (n=7). (C) qRT-PCR analysis of Ho-1 and (D) Thioredoxin Red and Gsr mRNA levels in untreated (n=12), PHZ- (n=6) and PHZ-Hx-treated Wt mice (n=5). (E) Representative M-mode echocardiogram of Wt mice at time 0 and 4 weeks after PHZ or PHZ and  $\alpha$ -tocopherol treatment. (F) Fractional shortening and (G) ejection fraction of PHZ- (n=6) mice and PHZ- $\alpha$ -tocopherol-treated mice (n=7) 4 weeks after the treatment. (H) Representative M-mode echocardiogram of Wt mice at time 0 and 4 weeks after PHZ or PHZ and Hx treatment. (I) Fractional shortening and (J) ejection fraction of PHZ- (n=12) and PHZ-Hx-treated mice (n=6) 4 weeks after the treatment. One-way analysis of variance with Bonferroni post-test analysis (A-D) and two-ways analysis of variance with Bonferroni post-test analysis (F-G, I-L) were performed. \*P < 0.05; \*\*P < 0.01; \*\*\*P < 0.001. Values represent mean  $\pm$  SEM.

**Figure 7. A model for Hx function in the heart.** In hemolytic conditions, non-hemopexin bound heme (NHBH) level rises up and (A) heme accumulates within cardiomyocytes perturbing heme/iron homeostasis and leading to ROS formation (cell on the left). ROS modify  $\text{Ca}^{2+}$ -handling proteins leading to altered  $\text{Ca}^{2+}$  fluxes within the cell (on the right). This ultimately results in impaired contraction. The treatment with antioxidants (NAC or  $\alpha$ -Tocopherol) rescues ROS-induced cardiomyocyte damage. (B) Hx, by scavenging NHBH, preserves both heme/iron and  $\text{Ca}^{2+}$  homeostasis. Our data suggest that in hemolytic disorders, plasma heme scavenging capacity might be increased by Hx administration thus limiting heme toxicity on the heart.

Figure 1

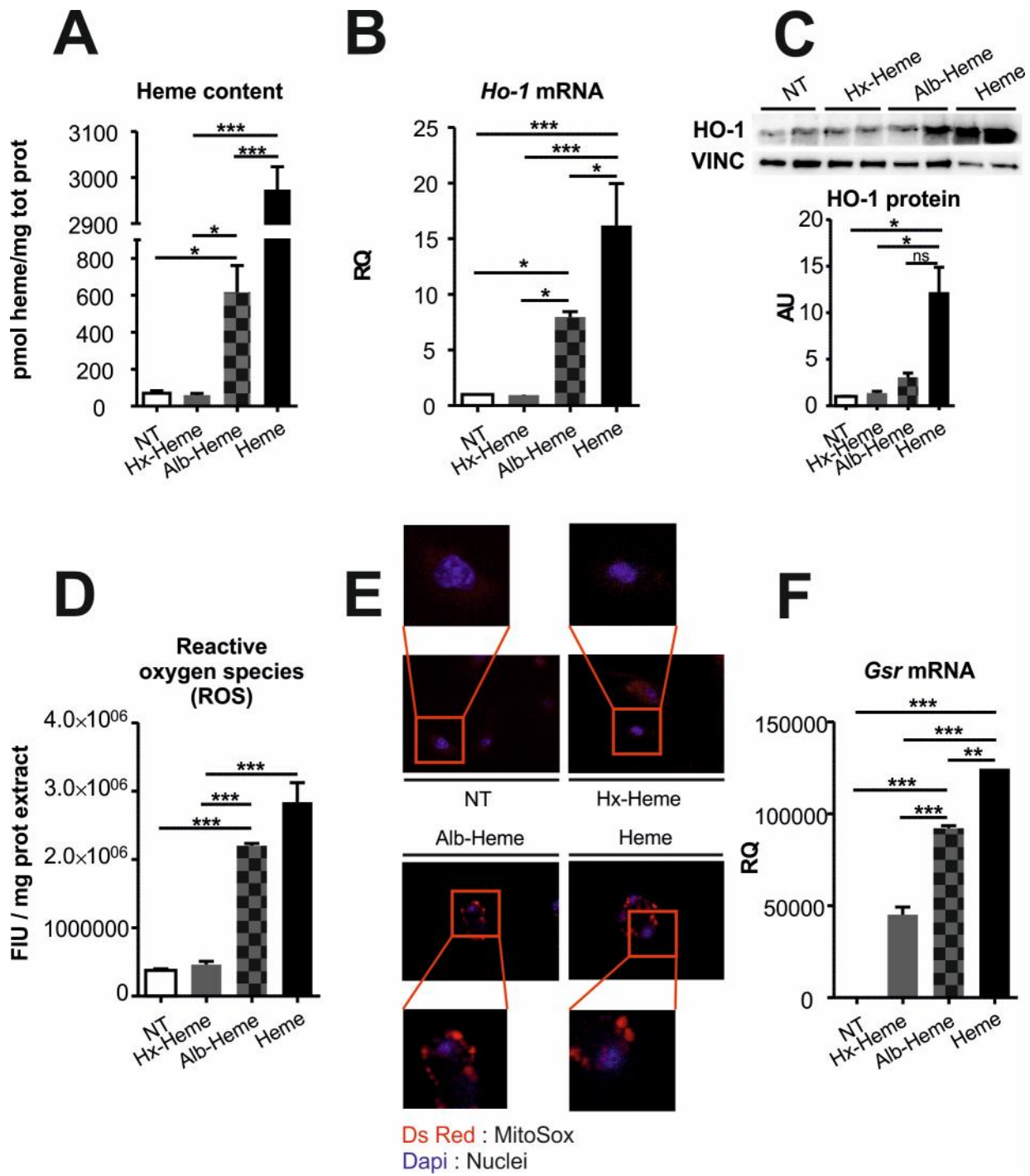


Figure 2

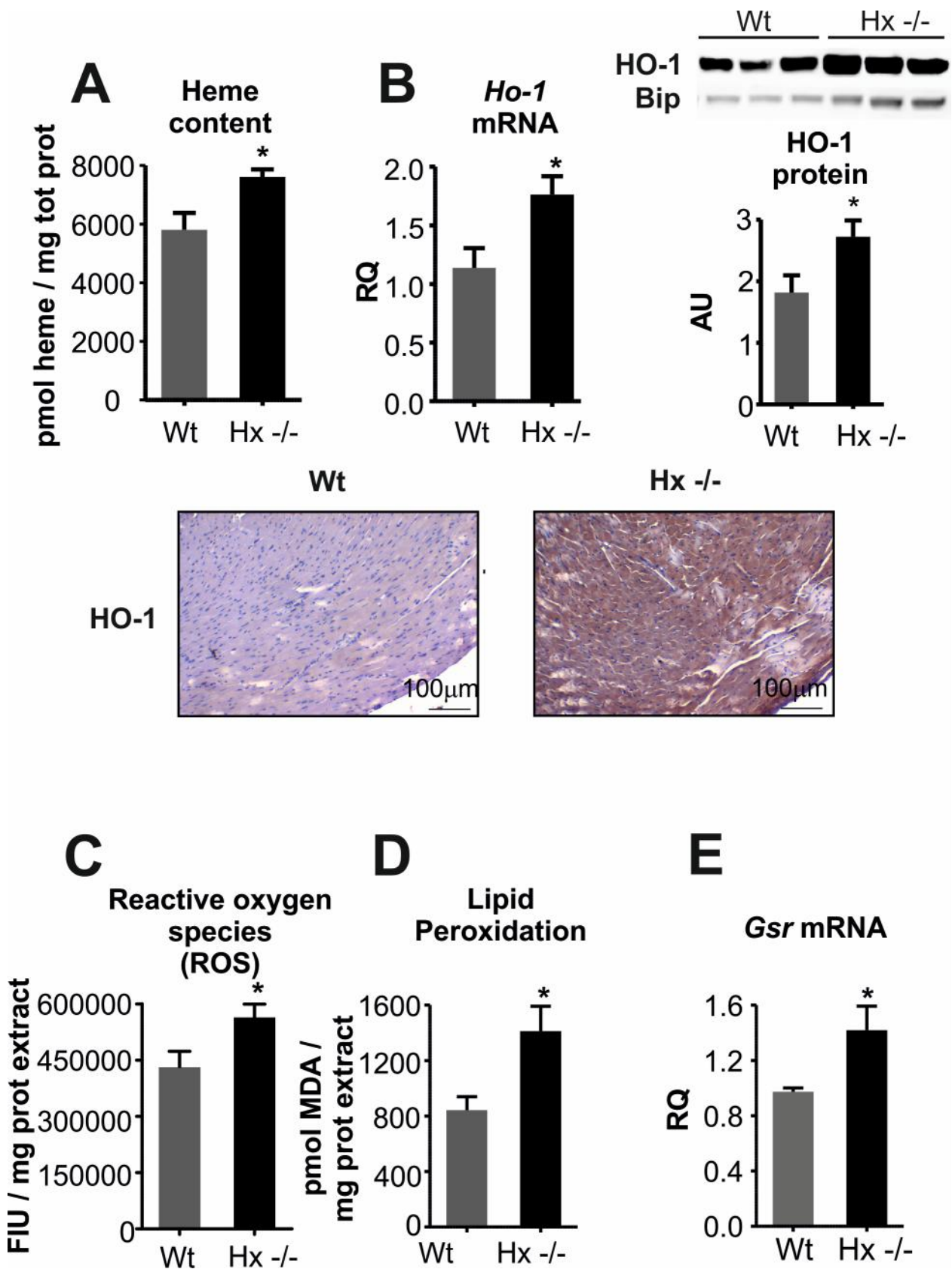




Figure 3

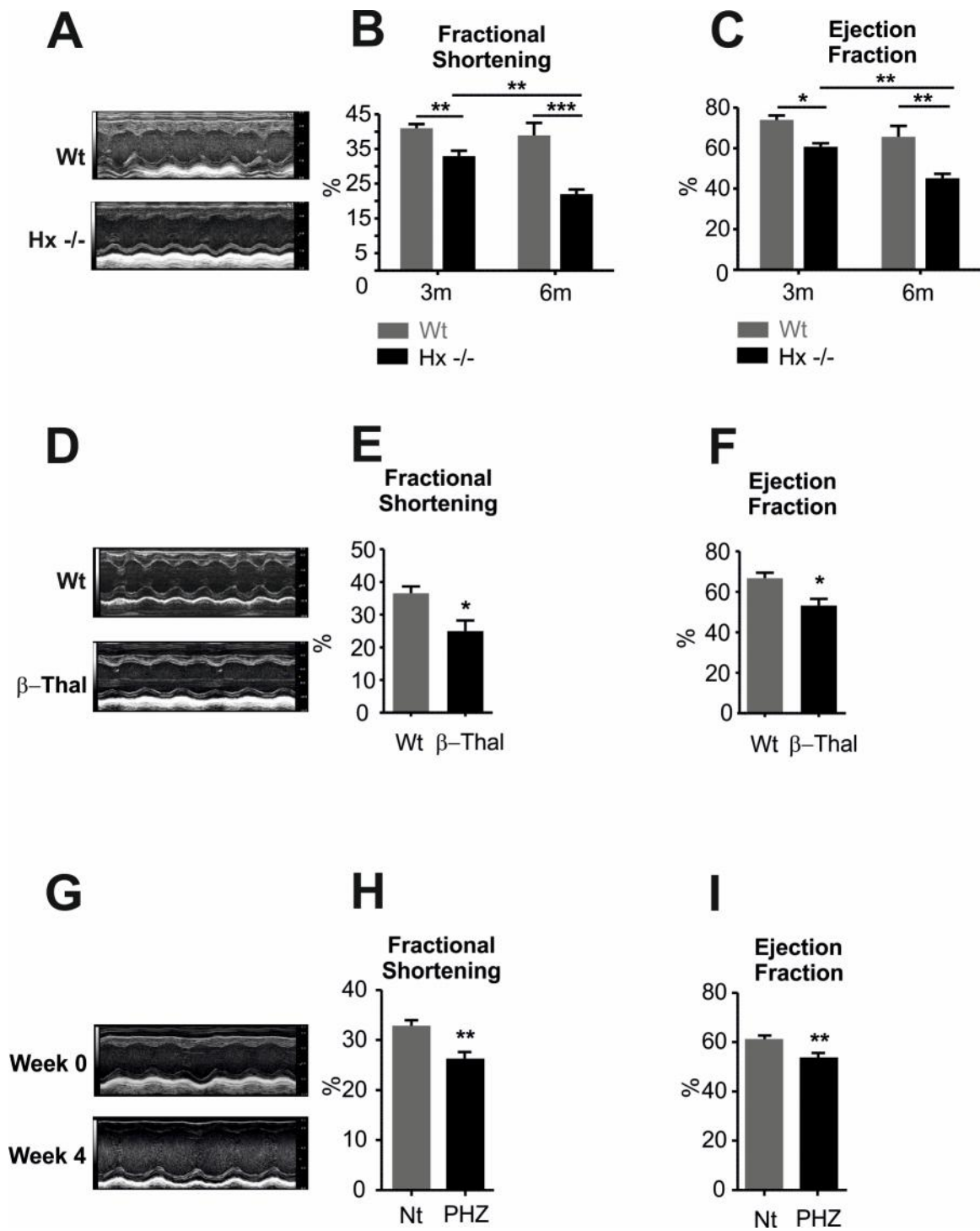


Figure 4

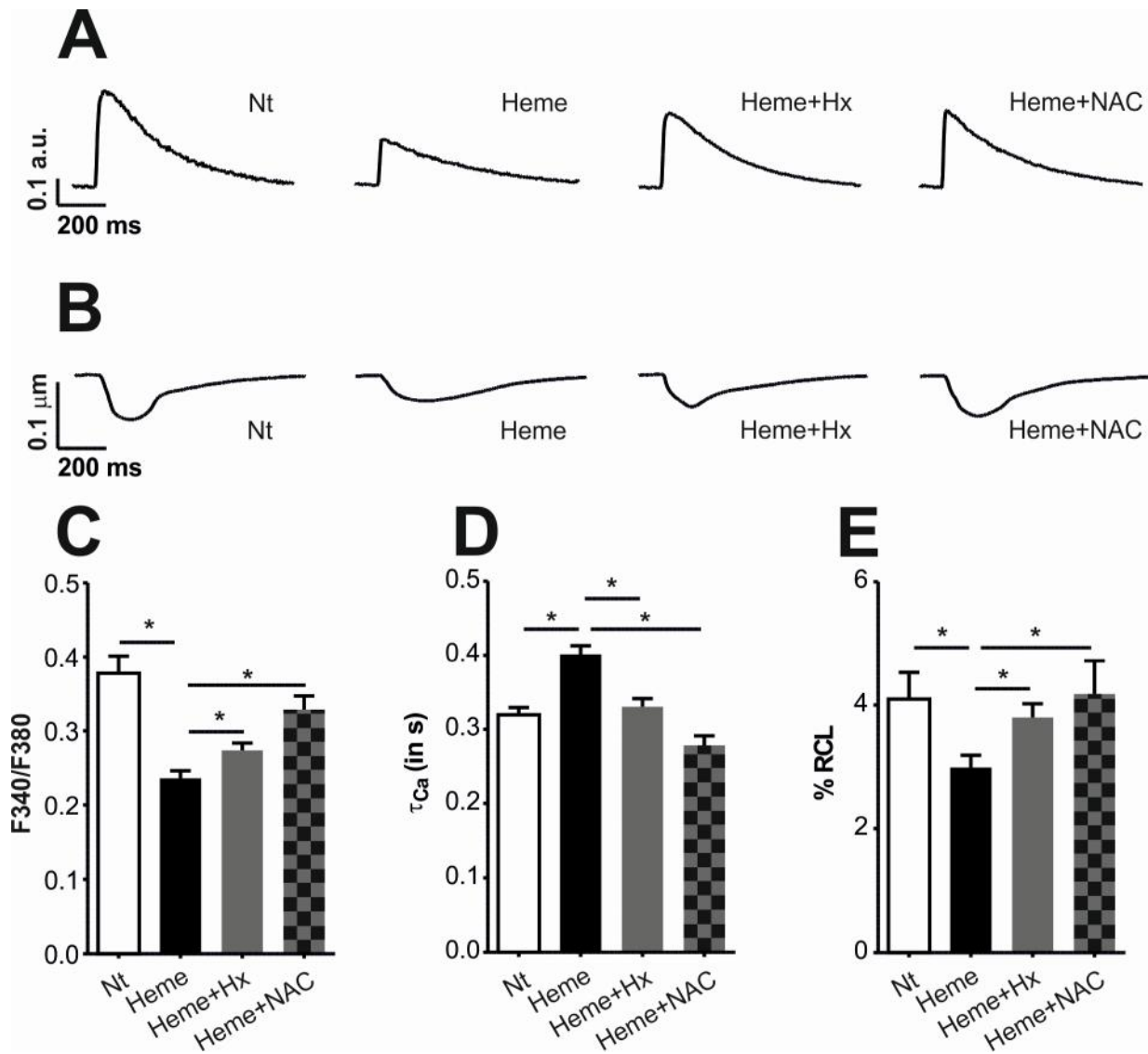


Figure 5

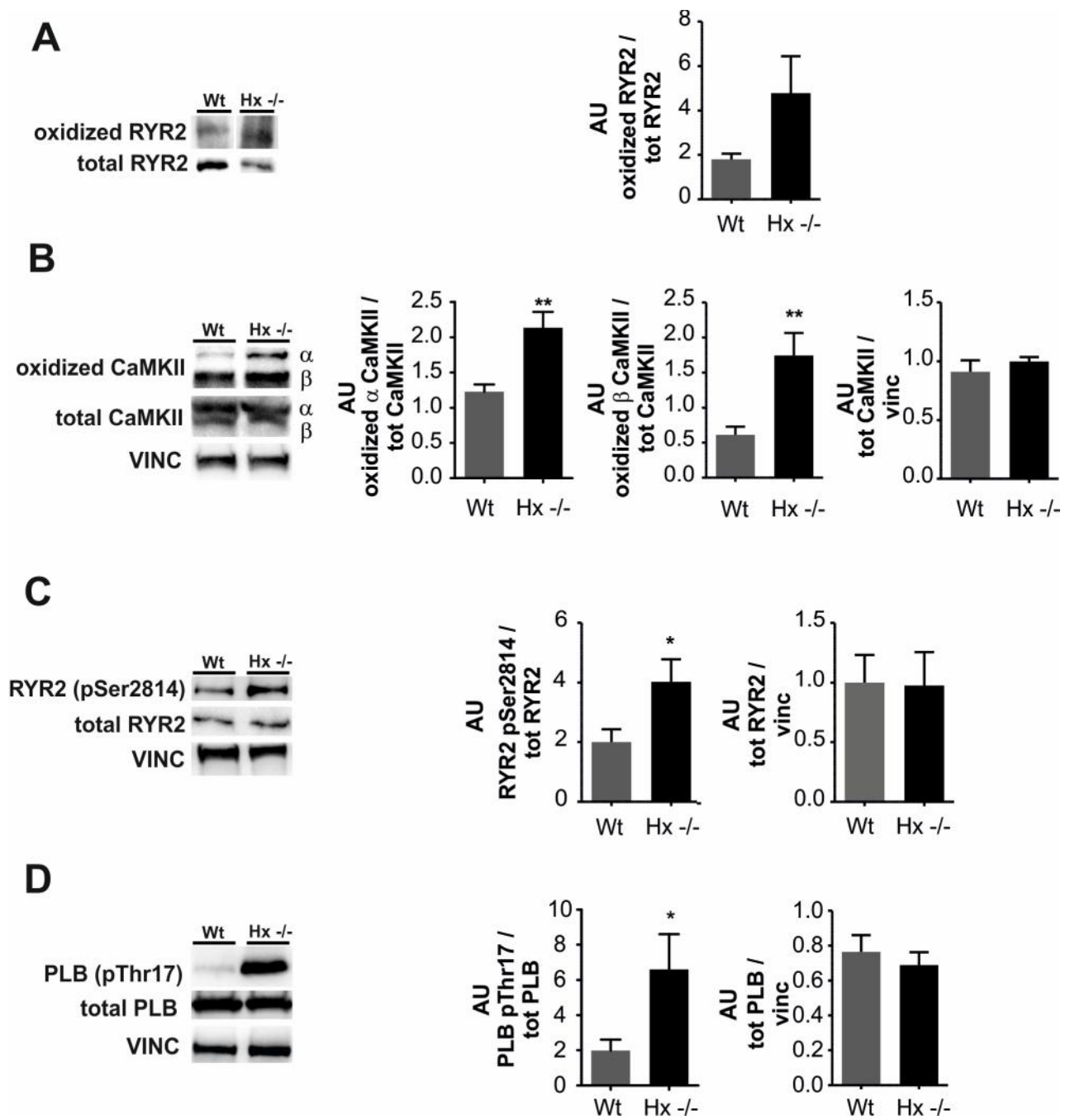


Figure 6

